

## Article

# Survival and Enrichment Analysis of Epithelial–Mesenchymal Transition Genes in Bladder Urothelial Carcinoma

Waleed Ali <sup>1,\*</sup>, Weirui Xiao <sup>1</sup>, Daniel Jacobs <sup>1</sup> and Andre Kajdacsy-Balla <sup>2</sup>

<sup>1</sup> Albert Einstein College of Medicine, New York, NY 10461, USA; weirui.xiao@einsteinmed.edu (W.X.); daniel.jacobs2@einsteinmed.edu (D.J.)

<sup>2</sup> Professor of Pathology, University of Illinois at Chicago College of Medicine, Chicago, IL 60607, USA; aballa@uic.edu

\* Correspondence: waleed.ali@einsteinmed.edu

**Abstract:** The escalating prevalence of bladder cancer, particularly urothelial carcinoma, necessitates innovative approaches for prognosis and therapy. This study delves into the significance of genes related to epithelial–mesenchymal transition (EMT), a process inherently linked to carcinogenesis and comparatively better studied in other cancers. We examined 1184 EMT-related gene expression levels in bladder urothelial cancer cases through the TCGA dataset. Genes shown to be differentially expressed in relation to survival underwent further network and enrichment analysis to uncover how they might shape disease outcomes. Our in silico analysis revealed a subset of 32 genes, including those significantly represented in biological pathways such as VEGF signaling and bacterium response. In addition, these genes interact with genes involved in the JAK-STAT signaling pathway. Additionally, some of those 32 genes have been linked to immunomodulators such as chemokines CCL15 and CCL18, as well as to various immune cell infiltrates. Our findings highlight the prognostic utility of various EMT-related genes and identify possible modulators of their effect on survival, allowing for further targeted wet lab research and possible therapeutic intervention.

**Keywords:** epithelial–mesenchymal transition; bladder urothelial carcinoma; TCGA; VEGF; in silico



**Citation:** Ali, W.; Xiao, W.; Jacobs, D.; Kajdacsy-Balla, A. Survival and Enrichment Analysis of Epithelial–Mesenchymal Transition Genes in Bladder Urothelial Carcinoma. *Genes* **2023**, *14*, 1899. <https://doi.org/10.3390/genes14101899>

Academic Editor: Anelia D. Horvath

Received: 28 August 2023

Revised: 16 September 2023

Accepted: 26 September 2023

Published: 30 September 2023



**Copyright:** © 2023 by the authors. Licensee MDPI, Basel, Switzerland. This article is an open access article distributed under the terms and conditions of the Creative Commons Attribution (CC BY) license (<https://creativecommons.org/licenses/by/4.0/>).

## 1. Introduction

Bladder cancer is the 10th most common malignancy worldwide with 573,278 new cases and 212,536 deaths in 2020 [1]. Urothelial carcinoma accounts for over 90% of bladder cancers, which costs the U.S. alone \$4 billion annually [2]. The prevalence is predicted to continue to rise due to the increasing industrialization and urbanization in developing countries, and the aging population [3,4]. Well-studied risk factors include cigarette smoking and occupational exposures especially in metal workers, painters, and chemical process workers [5,6]. Various altered genes have been implicated in amplifying the effect of these environmental exposures including carcinogen detoxification genes like *UDP Glucuronosyltransferase Family 1 Member A Complex Locus (UGT1A)* and *N-acetyltransferase 2 (NAT2)* [7–9], fibroblast growth factor receptor 3 (*FGFR 3*) [10], *p16*, *p53*, retinoblastoma (*RB*), matrix metalloproteinases, genes involved in folate metabolism, and high activity metabolic activators like high activity P450 cytochrome enzymes [11–17]. Within the TNM staging used, T1 represents tumor invasion up to the muscular layer of the bladder, with further stages T2,3,4 representing further progression into the muscle, perivesicular layer, and adjacent structures and organs, respectively. Currently, treatment options include transurethral resection of bladder tumor (TURBT) and intravesical therapy for non-muscle invasive, while options for metastatic disease include radial cystectomy, neoadjuvant chemotherapy, and newer immunotherapies [2,18–22].

Several genes have been implicated in the development of urothelial cancer and metastases and used as targets for therapy. Some of these include *LRP1B* [23], *ERRC2*, *FANCC*, *ATM*, *RB1* [24], *p53* [25], and *SLC14A1* [26]. There are currently no widely accepted

bladder cancer screening programs, though biannual cystoscopies have been found to be efficacious in vulnerable subpopulations [27–29]. Currently follow-up is time-consuming and expensive, consisting of cystoscopy, imaging, and surgery; urine biomarkers are being studied to supplement those options [18,19].

Cells involved in the invasion of bladder cancer alter their surroundings and can also become transiently and reversibly plastic, turning into mesenchymal stem cells. This is the epithelial–mesenchymal transition (EMT), which is among the most relevant paradigm shifts in how we view cancer progression and can combat its growth. During EMT, epithelial cells lose their polarized, adhesive characteristics and gain a mesenchymal phenotype, enabling them to migrate and invade surrounding tissues [30,31]. Transcription factors including Snail, Zeb, and Twist aid in this process by repressing E-cadherin, an epithelial transmembrane protein [32]. In contrast to epithelial cells, mesenchymal carcinoma cells exhibit specific metabolic needs. As they undergo EMT, cancer cells finely regulate multiple metabolic pathways to support the demands of rapid cell proliferation [33]. The molecular pathways shown to be associated with EMT include Snail/Slug, Twist, Six1, Cripto, TGF- $\beta$ , and Wnt/ $\beta$ -catenin [34]. The literature shows how genes such as *CDH1*, *ZEB1*, *TGFB*, *CDH2*, *VIM*, and *TIMP1* have been linked to inducing the EMT phenotype, driving cell migration, and adapting to changing demands on the primary tumor [33,35,36].

In bladder cancer, various microRNAs (miRNAs) have been found to regulate proteins such as Smad7 or Twist1, either promoting or disrupting EMT and metastasis [37]. Understanding the mechanisms underlying EMT is crucial for developing targeted therapies to control cancer metastasis and may prove useful in treatment options going forward. Comparatively, there has been less work in this field in bladder cancer than in other cancers. This paper examines a multitude of EMT-related genes in relation to not only outcomes, but also the biologic networks and pathways which allow these genes to influence carcinogenesis and affect these outcomes.

## 2. Materials and Methods

### 2.1. Selection of Genes

To have a comprehensive overview of genes involved in the epithelial–mesenchymal transition, dbEMT 2.0 (<http://dbemt.bioinfo-minzhao.org/> (accessed on 1 September 2022)), a database curated for focus on EMT-related genes, was utilized. A spreadsheet was generated with 1184 genes listed on the database, obtained from an initial PubMed abstract query for “Epithelial Mesenchymal Transition Genes” with the results mined for unique genes linked to EMT (see Supplemental Materials).

### 2.2. Survival Analysis

Publicly available cases from the NIH-funded “The Cancer Genome Atlas” (TCGA) project were utilized to examine gene expression pertaining to survival in bladder urothelial cancer (data portal: <https://portal.gdc.cancer.gov/projects/TCGA-BLCA> (accessed on 1 September 2022)). Kaplan–Meier plots were generated through the R2 platform (<https://hgservers1.amc.nl/cgi-bin/r2/main.cgi> (accessed on 1 September 2022)) using the TCGA dataset for “Bladder Urothelial Carcinoma”,  $n = 407$ . The built-in “KaplanScan” algorithm was used to divide mRNA gene expression into “high” versus “low” categories ( $n$  values for each based on KaplanScan groupings of expression). Overall survival was compared to follow-up time in months being analyzed. For multiple hypothesis testing,  $p$ -values were adjusted to a false discovery rate (FDR) of 0.05.

### 2.3. Expression Analysis

To compare normal versus tumor levels of those EMT genes which showed differential expression regarding survival, mRNA levels for the “Bladder Urothelial Carcinoma” TCGA dataset were analyzed with a Welch’s  $t$ -test through the UCSC Xena platform. This platform is a genome browser and visualization tool of genomic and phenotypic data for both public and private datasets (<https://xena.ucsc.edu/> (accessed on 1 September 2022)). An

FDR cutoff of 0.05 was used for significance. Violin plots were generated to visualize expression values.

Through the aforementioned R2 platform, the expression levels of the previously mentioned genes which showed differential expression in regard to survival were analyzed. mRNA gene levels were compared in respect to pathologic staging and, given the small  $n$  associated with cases of stage 1 bladder urothelial cancer in the TCGA dataset ( $n = 2$ ), Kruskal–Wallis analysis with corresponding pairwise Welch’s  $t$ -tests were used. Again,  $p$ -values were adjusted and an FDR cutoff of 0.05 was used.

#### 2.4. Network & Enrichment Analysis

GeneMANIA (<http://www.genemania.org> (accessed on 1 September 2022)) serves as a platform for visualizing diverse biological interactions encompassing co-expression, co-localization, and domain similarity. In this study, GeneMANIA, R (<https://www.r-project.org/> (accessed on 1 September 2022)), and the Cytoscape platform (<https://cytoscape.org/> (accessed on 1 September 2022)) were utilized to construct a gene–gene interaction network focusing on EMT-related genes exhibiting significant differential expression based on survival data.

Subsequently, the network analysis highlighted certain genes alongside the aforementioned EMT genes. These genes underwent enrichment analysis to shed light on their potential involvement in specific biological processes, using annotations from the Gene Ontology (GO), Kyoto Encyclopedia of Genes, and Genomes (KEGG) databases. It was carried out through the Metascape platform (<http://metascape.org> (accessed on 1 October 2022)). The criteria for this analysis included a minimum overlap of 3 genes and an enrichment threshold of 1.5. Statistical significance was set at  $p < 0.05$ .

#### 2.5. Tumor Immune Microenvironment Analysis

The relationship between the EMT-related genes differentially expressed in connection with survival and the immune system in cases of bladder urothelial cancer was examined through the TISIDB and TIMER platform. Spearman’s correlations between mRNA gene expression of the EMT genes and clinically relevant immunoinhibitor and cytokine gene expressions were calculated and visualized. Those with a rho of  $>|0.40|$  were considered meaningful with a  $p$ -value of  $>0.01$ . Devolution methods were used to estimate the immune infiltration of a wide variety of immune cells based on gene expression on the TIMER platform. The Spearman’s correlation was adjusted based on tumor purity, with a rho of  $>|0.30|$  visualized.

### 3. Results

#### 3.1. Survival Analysis

A myriad of EMT-related genes showed differential expression in normal versus cancer tissues. Kaplan–Meier plots (Figure 1) were generated using TCGA data on “Bladder Urothelial Carcinoma” for each of the 1184 genes mined from the EMTdb, with only 32 meeting significant cutoff following FDR correction (Table 1).

#### 3.2. Expression Analysis

Out of the 32 genes highlighted in the survival analysis, some of them also showed statistically significant expression levels when comparing normal versus tumor samples. This can be seen in the density plot (Figure 2) or in more detail in the sample violin plots (Figure 3); the rest of the genes and  $p$ -values from the violin plots in Supplemental Materials can be seen in Table 4. Some genes also showed significant differential expression based on tumor stage (Figure 4).

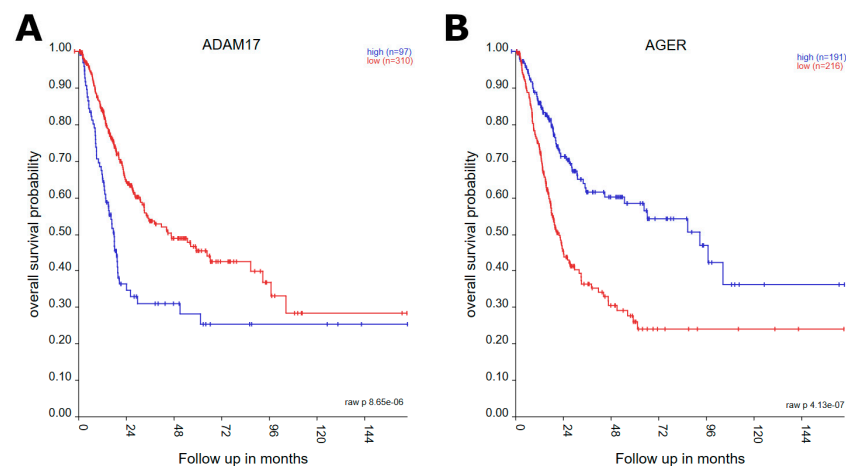


**Figure 1.** Subset of Kaplan–Meier plots based on mRNA expression of EMT-related genes which showed to be differentially expressed in relation to overall survival. Each plot lists the numbers of pts in “high” versus “low” mRNA expression cohorts based on the KaplanScan grouping algorithm. (A,B) show subset of Kaplan–Meier plots, based on gene expression levels of *ADAM17* and *ADER* respectively. See Supplemental Figure S1 for Kaplan–Meier plots of all genes shown to be differentially expressed.

**Table 1.** Tabulated data from Kaplan–Meier plots based on mRNA expression of EMT-related genes which showed to be differentially expressed in regard to overall survival.

Gene	p-Value	Expression in Worse Prognosis
<i>ADAM17</i>	$8.65 \times 10^{-6}$	low
<i>AGER</i>	$4.13 \times 10^{-7}$	high
<i>ANXA1</i>	$1.80 \times 10^{-6}$	low
<i>ARMC8</i>	$3.99 \times 10^{-8}$	low
<i>ART1</i>	$1.36 \times 10^{-3}$	high
<i>BBC3</i>	$5.28 \times 10^{-6}$	high
<i>CEMIP</i>	$1.83 \times 10^{-5}$	low
<i>ELSPBP1</i>	$1.65 \times 10^{-3}$	high
<i>FBP1</i>	$3.43 \times 10^{-5}$	high
<i>FN1</i>	$1.11 \times 10^{-5}$	low
<i>FOXA1</i>	$8.51 \times 10^{-5}$	high
<i>HOOK1</i>	$4.71 \times 10^{-12}$	high
<i>HTN1</i>	$1.02 \times 10^{-3}$	high
<i>IL22</i>	$4.18 \times 10^{-4}$	high
<i>INPP4B</i>	$2.37 \times 10^{-5}$	high
<i>LAMC2</i>	$1.98 \times 10^{-9}$	low
<i>LYPD3</i>	$3.33 \times 10^{-5}$	low
<i>MAP2K1</i>	$3.73 \times 10^{-7}$	low
<i>NES</i>	$2.91 \times 10^{-9}$	low
<i>NR2F2</i>	$1.34 \times 10^{-6}$	low
<i>NRP2</i>	$5.85 \times 10^{-5}$	low
<i>PDCD61P</i>	$1.31 \times 10^{-5}$	low
<i>PEBP4</i>	$2.16 \times 10^{-4}$	high
<i>PRKCI</i>	$2.65 \times 10^{-4}$	low
<i>PTPN6</i>	$2.03 \times 10^{-7}$	high
<i>RUNX2</i>	$7.19 \times 10^{-8}$	low
<i>SCEL</i>	$2.27 \times 10^{-7}$	low
<i>SLC9A3R1</i>	$3.78 \times 10^{-4}$	low
<i>SOX3</i>	$3.92 \times 10^{-4}$	high
<i>SPRR2A</i>	$1.17 \times 10^{-5}$	low
<i>STIM2</i>	$2.11 \times 10^{-11}$	high
<i>TBX3</i>	$2.50 \times 10^{-4}$	high

Genes with “high” mRNA expression leading to worse prognosis include those in Table 2.

**Table 2.** List of genes and *p*-values for which high mRNA expression is correlated with worse prognosis.

Gene	<i>p</i> -Value
<i>ADAM17</i>	0.0182
<i>ANXA1</i>	0.0433
<i>ARMC8</i>	0.0009
<i>CEMIP</i>	0.0300
<i>FN1</i>	0.0443
<i>LAMC2</i>	0.0050
<i>LYPD3</i>	0.0461
<i>MAP2K1</i>	0.0419
<i>NES</i>	0.0413
<i>NR2F2</i>	0.0495
<i>NRP2</i>	0.0481
<i>PDCD6IP</i>	0.0311
<i>PRKCI</i>	0.0457
<i>RUNX2</i>	0.0007
<i>SCEL</i>	0.0018
<i>SLC9A3R1</i>	0.0467
<i>SPRR2A</i>	0.0342

On the other hand, genes which showed “low” mRNA expression leading to worse prognosis include those in Table 3.

**Table 3.** List of genes and *p*-values for which low mRNA expression is correlated with worse prognosis.

Gene	<i>p</i> -Value
<i>AGER</i>	0.0441
<i>ART1</i>	0.0446
<i>BBC3</i>	0.0317
<i>ELSPBP1</i>	0.0486
<i>FBP1</i>	0.0359
<i>FOXA1</i>	0.0356
<i>HOOK1</i>	0.0011
<i>HTN1</i>	0.0478
<i>IL22</i>	0.0389
<i>INPP4B</i>	0.0314
<i>PEBP4</i>	0.0322
<i>PTPN6</i>	0.0137
<i>SOX3</i>	0.0324
<i>STIM2</i>	0.0500
<i>TBX3</i>	0.0482

**Table 4.** Violin plot genes and *p*-values.

Gene	<i>p</i> -Value	Higher Expression
<i>ADAM17</i>	$8.31 \times 10^{-4}$	Primary tumor
<i>AGER</i>	$2.77 \times 10^{-2}$	Primary tumor
<i>ANXA1</i>	$1.41 \times 10^{-2}$	Normal tissue
<i>ARMC8</i>	$2.35 \times 10^{-4}$	Normal tissue
<i>ART1</i>	$1.73 \times 10^{-1}$	Normal tissue
<i>BBC3</i>	$5.39 \times 10^{-5}$	Primary tumor

Table 4. Cont.

Gene	p-Value	Higher Expression
<i>CEMIP/KIAA1199</i>	$1.93 \times 10^{-3}$	Primary tumor
<i>ELSPBP1</i>	$2.52 \times 10^{-1}$	Normal tissue
<i>FBP1</i>	$7.76 \times 10^{-1}$	Normal tissue
<i>FN1</i>	$3.88 \times 10^{-1}$	Primary tumor
<i>FOXA1</i>	$1.64 \times 10^{-1}$	Primary tumor
<i>HOOK1</i>	$5.13 \times 10^{-3}$	Primary tumor
<i>IL22</i>	$9.30 \times 10^{-2}$	Normal tissue
<i>INPP4B</i>	$2.06 \times 10^{-2}$	Primary tumor
<i>LAMC2</i>	$1.05 \times 10^{-4}$	Primary tumor
<i>LYPD3</i>	$3.03 \times 10^{-1}$	Primary tumor
<i>MAP2K1</i>	$2.88 \times 10^{-3}$	Primary tumor
<i>NES</i>	$8.36 \times 10^{-8}$	Normal tissue
<i>NR2F2</i>	$3.04 \times 10^{-1}$	Normal tissue
<i>NRP2</i>	$1.24 \times 10^{-4}$	Normal tissue
<i>PDCD6IP</i>	$3.67 \times 10^{-1}$	Primary tumor
<i>PEBP4</i>	$2.17 \times 10^{-4}$	Normal tissue
<i>PRKCI</i>	$4.31 \times 10^{-3}$	Primary tumor
<i>PTPN6</i>	$3.14 \times 10^{-3}$	Primary tumor
<i>RUNX2</i>	$1.90 \times 10^{-2}$	Primary tumor
<i>SCEL</i>	$2.05 \times 10^{-1}$	Primary tumor
<i>SLC9A3R1</i>	$8.95 \times 10^{-3}$	Primary tumor
<i>SOX3</i>	$3.35 \times 10^{-2}$	Normal tissue
<i>SPRR2A</i>	$2.77 \times 10^{-1}$	Primary tumor
<i>STIM2</i>	$8.06 \times 10^{-1}$	Normal tissue
<i>TBX3</i>	$7.13 \times 10^{-1}$	Primary tumor

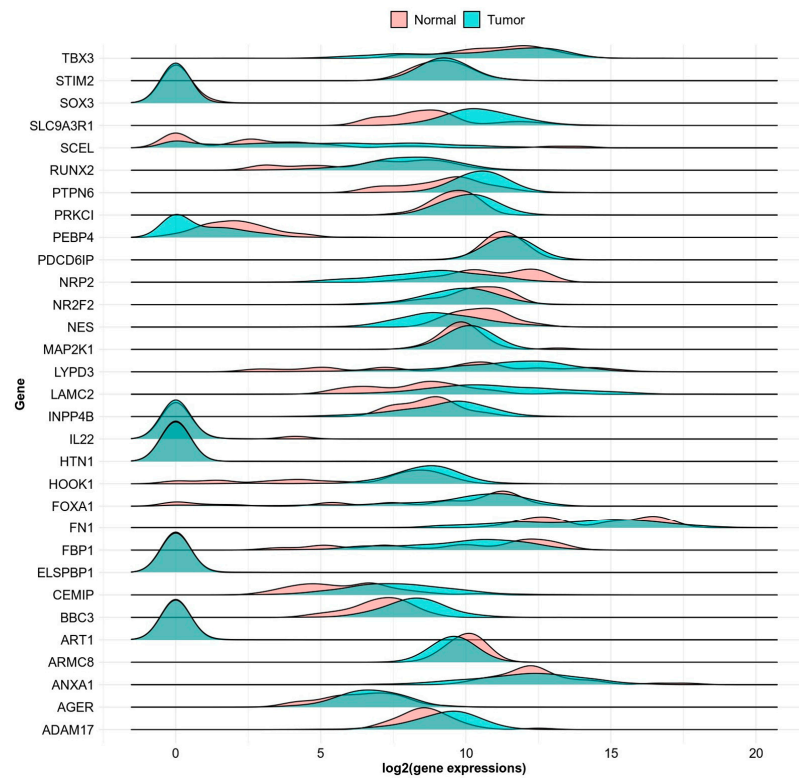
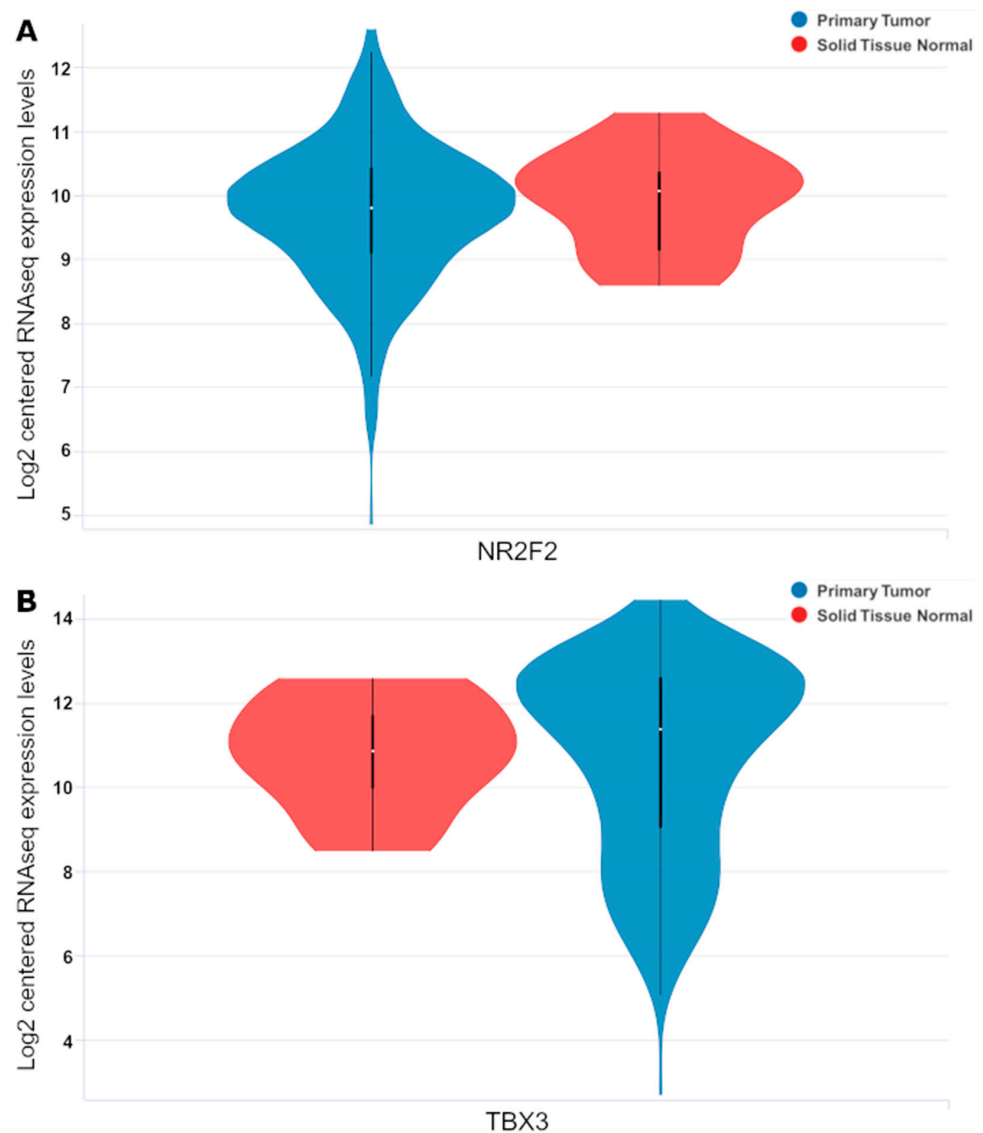


Figure 2. Density plot showing expression of normal versus tumor expressions for all selected genes which had both TCGA and GTEX data.



**Figure 3.** Subset of violin plot showing mRNA expression between primary tumors (Blue,  $n = 407$ ) and surrounding normal tissue (Red,  $n = 19$ ). For full listing, see Supplemental Figure S2. (A,B) show subset of violin plots, showing primary versus normal solid tissue violin plots for *NR2F2* and *TBX3* respectively.

From the XENA browser, 19 normal tissues were compared with 407 TCGA cases. Following FDR correction (cut-off  $p$ -value is 0.003143), 10 genes were shown to be differentially expressed when considering overall survival (Table 5).

Several genes approach significance post-correction (Table 6).

Out of the same set of EMT-genes regarding survival, 10 out of the 32 showed differential expression when considering pathologic staging (Table 7).

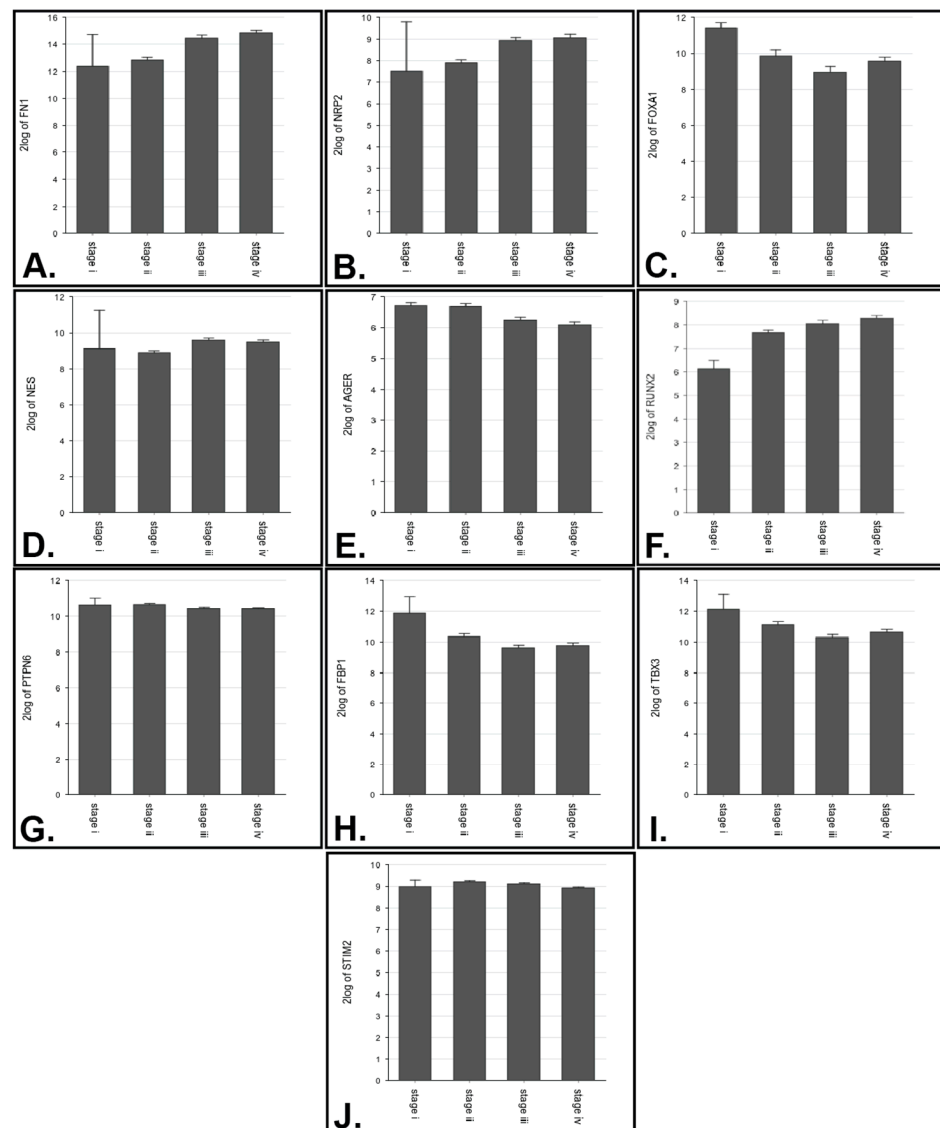


**Figure 4.** Bar plots showing log2 median mRNA expression levels of the EMT-survival related genes which also showed significant differences between any of the stages (Stage 1  $n = 2$ , Stage 2  $n = 130$ , Stage 3  $n = 140$ , Stage 4  $n = 134$ ). (A–J) show genes for which expression levels were significantly different (stage plots of *FN1*, *NRP2*, *FOXA1*, *NES*, *AGER*, *RUNX2*, *PTPN6*, *FBP1*, *TBX3*, and *STIM2* respectively).

**Table 5.** List of genes differentially expressed regarding overall survival when comparing normal versus tumor samples with  $p$ -values.

Gene	$p$ -Value
<i>ADAM17</i>	0.0008
<i>ARMC8</i>	0.0002
<i>BBC3</i>	0.0001
<i>CEMIP</i>	0.0019
<i>LAMC2</i>	0.0001
<i>MAP2K1</i>	0.0029
<i>NES</i>	<0.0001
<i>NRP2</i>	0.0001
<i>PEBP4</i>	0.0002
<i>PTPN6</i>	0.0031

**Table 6.** List of genes that approach significance after FDR correction with *p*-values (cutoff *p* value is 0.003143).

Gene	<i>p</i> -Value
<i>HOOK1</i>	0.0051
<i>HTN1</i>	0.0069
<i>SLC9A3R1</i>	0.0090

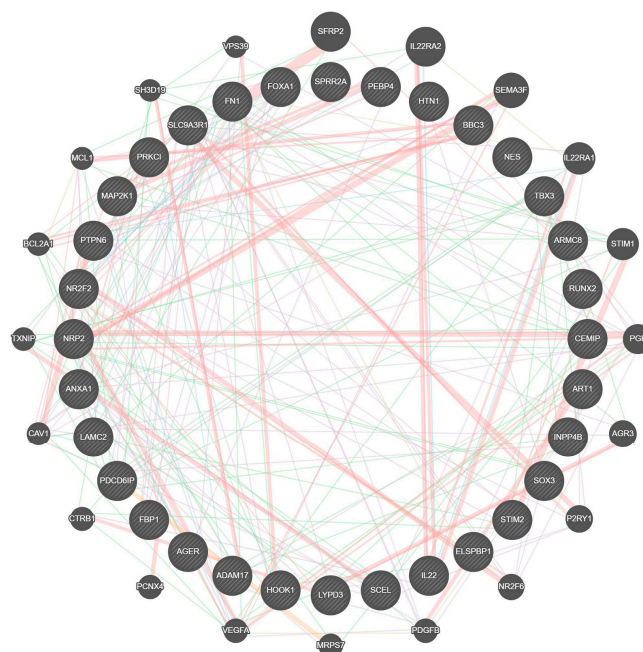
**Table 7.** List of stages that showed significantly different expression of the relevant gene based off TCGA datasets.

Gene	Different Stages
<i>FN1</i>	2 vs. 3 ( $p = 1.22 \times 10^{-8}$ ), 2 vs. 4 ( $4.20 \times 10^{-12}$ )
<i>NRP2</i>	2 vs. 4 ( $p = 2.10 \times 10^{-8}$ )
<i>FOXA1</i>	1 vs. 3 ( $p = 5.08 \times 10^{-3}$ )
<i>NES</i>	2 vs. 3 ( $p = 1.71 \times 10^{-5}$ )
<i>AGER</i>	2 vs. 3 ( $p = 2.00 \times 10^{-3}$ ), 2 vs. 4 ( $p = 2.39 \times 10^{-5}$ )
<i>RUNX2</i>	2 vs. 4 ( $p = 2.99 \times 10^{-4}$ )
<i>PTPN6</i>	2 vs. 4 ( $p = 7.24 \times 10^{-3}$ )
<i>FBP1</i>	2 vs. 3 ( $p = 5.65 \times 10^{-3}$ )
<i>TBX3</i>	2 vs. 3 ( $p = 3.56 \times 10^{-3}$ )
<i>STIM2</i>	2 vs. 4 ( $p = 3.97 \times 10^{-5}$ )

### 3.3. Identification of Further Gene Interactions and Enriched Biological Processes

#### 3.3.1. Network Analysis

Network analysis was employed to identify genes with interconnected relationships, utilizing factors such as physical interactions, co-localization, and co-expression data (Figure 5). The genes chosen for constructing each network analysis were the previously mentioned EMT-associated genes that displayed distinct expression patterns in survival outcomes.

**Figure 5.** Network analysis showing 20 of the most highlighted genes. The analysis was conducted utilizing factors such as physical and anticipated interactions, protein co-localization, and shared DNA domains, alongside various other attributes. Connections between genes based on physical interactions are highlighted in red, shared pathways in blue, shared protein domains in yellow, predicted in orange, co-expression in purple, genetic interactions in green, and co-localization in navy.

### 3.3.2. Enrichment Analysis

Enrichment analysis was executed on two distinct gene sets: first, on the genes pinpointed in the network analysis, and additionally, on the genes situated at the periphery (“outer rim”) of the network analysis, apart from the initial EMT genes (Figure 6). Enrichment analysis of the initial 32 highlighted EMT genes showed numerous pathways significantly overrepresented in the cohort of genes, such as endothelial cell migration and regulation of cell shape, in line with the known physiologic processes involved with the epithelial–mesenchymal transition. However, other less canonically associated ones such as defense response to bacterium and carbohydrate response were also uncovered through the analysis. Regarding the genes listed in the network analysis, similar biologic processes such as the VEGFA signaling pathway was highlighted alongside other related ones such as HIF-1 survival signaling.

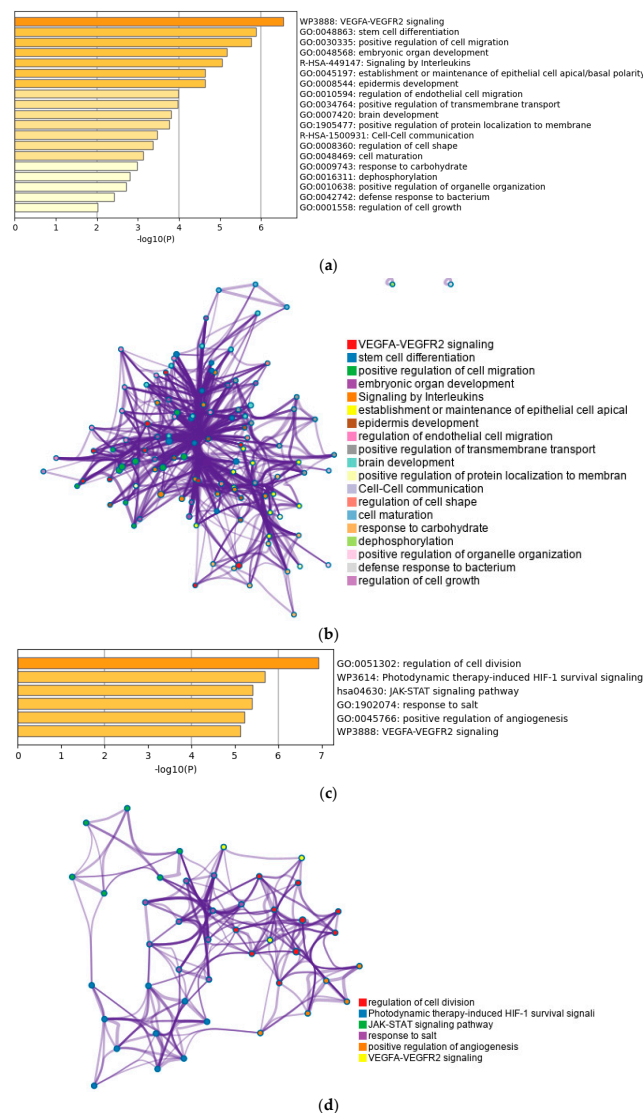


**Figure 6.** Enrichment analysis of the EMT genes involved in survival (a) as well as enrichment analysis highlighted in the aforementioned network analysis (b). Labeled are statistically enriched terms which are biologic pathways selected from KEGG and other hallmark gene sets. Additionally, for both the EMT genes and network highlighted gene ((c) and (d), respectively), the representative terms were converted into a network layout with each circle representing a single biologic process, grouped into larger “themes” as labeled in the color key. The size of the circle represents the amount of analyzed genes within that term.

### 3.4. Correlation to Inflammation Mediators

#### 3.4.1. Immunomodulator, Cytokine

Through examining for correlation between various immunomodulators and chemokines (see Appendix A, Table A1 for list), the following plots were generated (Figure 7), with the statistically and clinically significant ones ( $p < 0.05$  post correction,  $|\rho| > 0.4$ ) being shown. Out of the 32 genes, 12 were shown to have at least significant correlation with an immunomodulator or chemokines (TBX3, NRP2, FN1, FOXA1, FBP1, ANXA1, LAMC2, HOOK1, NES, PTPN6, RUNX2), with the first four having at least 25 different immunomodulators or cytokines to be significantly correlated with (Table 8).

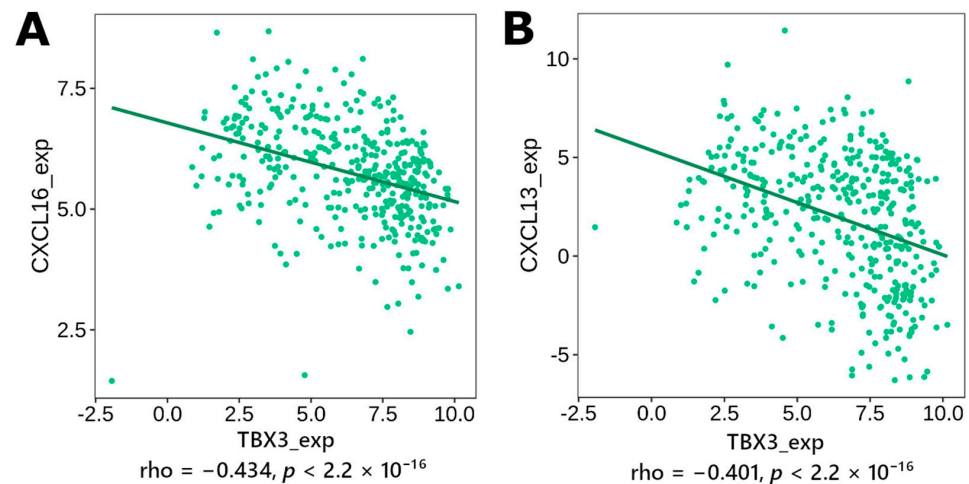


**Figure 7.** Sample Spearman's correlation graphs for *TBX3* (full table of all EMT-related genes in Appendix A, Table A2), grouped by EMT-gene of interest. Only correlations shown to be statistically significant ( $p < 0.05$  post multiple hypothesis correction) and deemed clinically significant  $|\rho| > 0.4$  are depicted both in the figure and included in the summary below. Subset shown, with (A) showing *TBX3* expression correlation with *CXCL16* expression and (B) showing correlation between *TBX3* and *CXCL13* expression; for other genes *NRP2*, *FN1*, *FOXA1*, *FBP1*, *ANXA1*, *LAMC2*, *HOOK1*, *NES*, *RUNX2*, and *PTPN6* see Supplemental Figure S3.

**Table 8.** Summary of Spearman's correlation data between EMT-related gene and various immunomodulators, grouped by EMT-gene of interest.

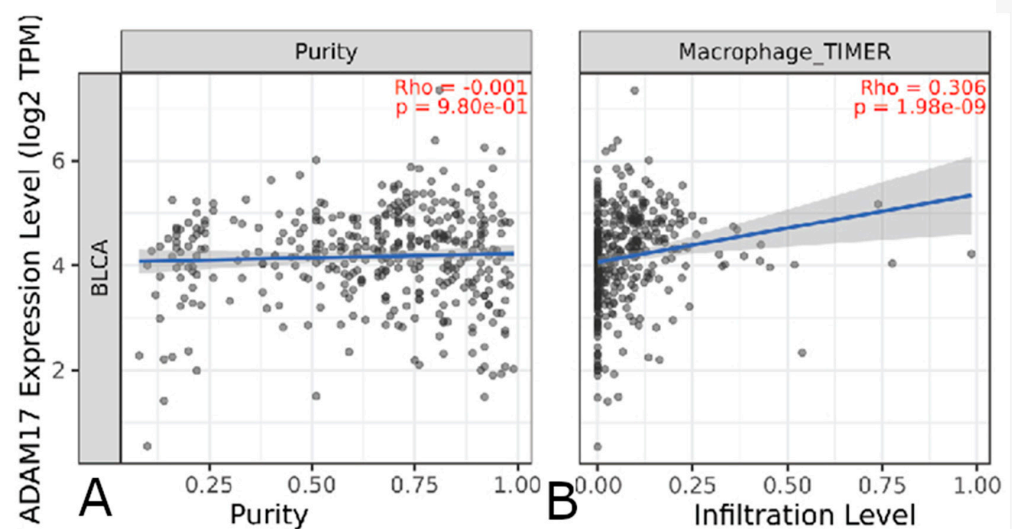
Gene	Immunomodulator (Positive Correlation)	Immunomodulator (Negative Correlation)
<i>TBX3</i>		<i>CXCL16</i> , <i>CXCL13</i> , <i>CXCL11</i> , <i>CXCL10</i> , <i>CXCL9</i> , <i>CXCL5</i> , <i>CXCL3</i> , <i>CXCL2</i> , <i>CXCL1</i> , <i>CCL26</i> , <i>CCL23</i> , <i>CCL18</i> , <i>CCL13</i> , <i>CCL8</i> , <i>CCL7</i> , <i>CCL5</i> , <i>CCL4</i> , <i>CCL3</i> , <i>TIGIT</i> , <i>TGFB1</i> , <i>PDCD1LG2</i> , <i>PDCD1</i> , <i>LAG3</i> , <i>IL10</i> , <i>IDO1</i> , <i>HAVCR2</i> , <i>CTLA4</i> , <i>CSF1R</i> , <i>CD274</i>
<i>NRP2</i>	<i>CXCL13</i> , <i>CXCL12</i> , <i>CXCL11</i> , <i>CXCL10</i> , <i>CXCL9</i> , <i>CXCL2</i> , <i>CCL26</i> , <i>CCL23</i> , <i>CCL21</i> , <i>CCL19</i> , <i>CCL18</i> , <i>CCL13</i> , <i>CCL11</i> , <i>CCL8</i> , <i>CCL7</i> , <i>CCL5</i> , <i>CCL4</i> , <i>CCL3</i> , <i>CCL2</i> , <i>LAG3</i> , <i>TIGIT</i> , <i>TGFB1</i> , <i>PDCD1LG2</i> , <i>PDCD1</i> , <i>IL10</i> , <i>HAVCR2</i> , <i>CTLA4</i> , <i>CSF1R</i> , <i>BTLA</i> , <i>ADORA2A</i>	
<i>FN1</i>	<i>TGFB1</i> , <i>TGFB1</i> , <i>PDCD1LG2</i> , <i>LAG3</i> , <i>IL10</i> , <i>HAVCR2</i> , <i>CSF1R</i> , <i>CD274</i> , <i>CXCL13</i> , <i>CXCL12</i> , <i>CXCL11</i> , <i>CXCL10</i> , <i>CXCL9</i> , <i>CXCL5</i> , <i>CXCL2</i> , <i>CCL26</i> , <i>CCL23</i> , <i>CCL21</i> , <i>CCL18</i> , <i>CCL13</i> , <i>CCL11</i> , <i>CCL7</i> , <i>CCL5</i> , <i>CCL4</i> , <i>CCL3</i> , <i>CCL2</i>	

Table 8. Cont.

Gene	Immunomodulator (Positive Correlation)	Immunomodulator (Negative Correlation)
FOXA1	CCL15	CXCL12, CXCL11, CXCL10, CXCL9, CXCL5, CXCL3, CXCL2, CCL26, CCL23, CCL21, CCL18, CCL13, CCL8, CCL7, CCL5, CCL4, CCL3, CCL2, TGFB1, TGFB1, PDCD1LG2, LAG3, IL10, HAVCR2, CTLA4, CSF1R, CD274
FBP1	CCL15	CCL4, TGFB1, PDCD1LG2, CD274
ANXA1	PDCD1LG2, CD274, CCL7	
SPRR2A	CXCL8, TGFB1	
LAMC2	CXCL8, CXCL1, TGFB1	
HOOK1	TGFB1, CSF1R, CCL23	
NES	CXCL12, KDR	
PTPN6	LGAGLS9	
RUNX2	PDCD1LG2	

### 3.4.2. Immune Cell Infiltrate

Through the TIMER platform, deconvolution methods were used to estimate the amount of various immune cells (T cells CD4+, Tregs, B cells, Neutrophils, Monocytes, Macrophages, DCs, NK and Mast Cells; see Figure 8). Out of the 32 initial genes, 14 (ADAM17, AGER, ANXA1, ARMC8, FBP1, FN1, FOXA1, LAMC2, MAP2K1, NRP2, PTPN6, RUNX2, STIM2, TBX3) showed to have at least significant correlation (Spearman's correlation > 0.05 following adjustment based on tumor purity, with a rho of > |0.30|; see Table 9).



**Figure 8.** Correlations of various gene expression levels to tumor purity and immune infiltration. Only correlations to immune infiltration shown to be statistically significant ( $p < 0.05$  post multiple hypothesis correction) and deemed clinically significant  $|\text{rho}| > 0.3$  are depicted both in the figure and included in the summary below. Subset shown, for other genes *ANXA1*, *ARMC8*, *FBP1*, *FN1*, *FOXA1*, *LAMC2*, *MAP2K1*, *NRP2*, *PTPN6*, *RUNX2*, *STIM2*, *TBX3* see Supplemental Figure S2. (A) shows correlation between *ADAM17* gene expression and tumor purity (amount of non-cancerous cells in tumor sample) and (B) shows correlation between *ADAM17* expression level and calculated macrophage infiltration.

**Table 9.** Summary of Spearman’s correlation data between EMT-related gene and various immune cell types, grouped by EMT-gene of interest.

Gene	Immune Infiltrates (Positive Correlation)	Immune Infiltrates (Negative Correlation)
<i>ADAM17</i>	Macrophage, Neutrophil	
<i>AGER</i>		T cell CD8+
<i>ANX1</i>	T cell CD8+, Neutrophil, Myeloid dendritic cell	
<i>ARMC8</i>	Macrophage	
<i>FBP1</i>		T cell CD8+, Neutrophil, Myeloid dendritic cell
<i>FN1</i>	T cell CD4+, T cell CD8+, Macrophage, Myeloid dendritic cell	
<i>FOXA1</i>	T cell CD4+	T cell CD8+, Myeloid dendritic cell
<i>LAMC2</i>	T cell CD8+, Neutrophil, Myeloid dendritic cell	
<i>MAP2K1</i>	T cell CD8+, Neutrophil	
<i>NRP2</i>	T cell CD8+, Macrophage, Myeloid dendritic cell	
<i>PTPN6</i>		B cell
<i>RUNX2</i>	T cell CD8+, Myeloid dendritic cell	
<i>STIM2</i>	T cell CD4+	
<i>TBX3</i>		T cell CD8+, T cell CD4+, Neutrophil, Myeloid dendritic cell

#### 4. Discussion

Overall, we see a robust cohort of EMT-related genes that are differentially expressed as pertaining to survival in bladder urothelial carcinoma. *RUNX2*, a gene most associated with cartilage production, has been linked to pancreatic cancer and to breast cancer progression through modulation of MicroRNAs and the metastasis-associated 1 (MTA1)/NuRD complex [38,39]. By activating the Wnt signaling pathway, *ARMC8* has been linked to increased invasion in cutaneous squamous cell carcinoma and lung cancer [40–42]. Also implicated in the Wnt pathway, as well as the VEGF pathway, *CEMIP* (formerly known as KIA1199) has emerged via immunohistochemical studies as a possible biomarker for a variety of cancers [43–45]. The phosphatase *INPP4B* is an inhibitor of the Wnt pathway; its knockout has been linked to increased proliferation [46]. Knockout or downregulation of the transcription factor gene *FOXA1* has also been linked to worse prognosis, altering the carcinogenic activity of the Snail/Twist1 axis in breast cancer as well as prostate cancer [47,48]. *TBX3* has been linked to breast and cervical cancer proliferation, but it also inhibits the activity of the YAP/TAZ signaling pathway involved with cellular regeneration and growth [49–51].

Of note, *PTPN6*, a tyrosine phosphatase, affects cell growth and carcinogenesis in both bladder and colon cancer. Interestingly, overexpression of *PTPN6* has been associated with worse prognosis and increased metastasis, while the opposite was seen in other studies [52,53]. Additionally, there were cases where our findings were incongruent with other cancers. *PEBP4* expression was correlated with metastasis in colorectal and breast cancer but is significantly associated with better outcomes in our analysis. *AGER* (advanced glycosylation end-product-specific receptor) was shown to be associated with increased cell migration in cervical cancer, but the opposite as per our analysis [54]. The pro-carcinogenic effect that *ART1* has in colorectal cancer was not seen in our Bladder TCGA analysis [55].

Interestingly enough, some of the genes shown to be differentially expressed in regard to survival were not differentially expressed when comparing normal tissue to tumor; nor did their expression correlate to pathologic staging. For the pathologic staging, only *FN1*,

*NRP2*, *FOXA1*, *NES*, *AGER*, *RUNX2*, *PTPN6*, *FBP1*, *TBX3*, and *STIM2* were shown to be significantly different.

While there may be differences in Stage I expression versus the other stages, our sample size ( $n = 2$ ) was too small to reliably detect any except for in the expression levels of *FOXA1*. Instead, many of the differences were seen between Stage 2 versus 3 and 4. Histopathologically, this correlates with the expansion of the cancer through the muscle with possible lymph node and systemic metastasis. During this process, the pro-mobility changes which accompany the EMT would be fully evident. Our findings were mostly consistent with the survival analysis results, such as with *RUNX2* which showed worse prognosis with higher levels, increasing expression from Stages 1 to 4.

Through the network analysis, we were able to see more genes through which the EMT-related genes can modulate and affect carcinogenesis. For example, *VEGFA* was indicated, a well-known member of a family of growth factors which has proliferative and anti-apoptotic effects [56]. It has been found to be highly expressed in hepatocellular carcinoma (HCC) and triple-negative breast cancer (TNBC). It is associated with worse prognosis in HCC [57] and significantly lower progression-free survival in TNBC treated with chemotherapy [58]. Additionally, *SFRP2* was implicated, and recent immunohistochemistry work has linked this gene as a possible early biomarker of pancreatic and colon cancer [59,60]. Another gene highlighted in our analysis, *CAVI*, codes for a scaffolding protein and often predicts poor prognosis [61].

Enrichment analysis of the EMT-related genes further highlights the multiple modalities through which the EMT process itself encourages cancer growth and metastasis. Included among the highlighted cellular processes in our analysis are those regarding the establishment or maintenance of epithelial cell apical/basal polarity and positive regulation of cell migration. The VEGFA-VEGFR2 signaling pathway and associated angiogenesis, among the seminal hallmarks of cancer, were highlighted as the most overly enriched biologic process ( $p < 5.0 \times 10^{-7}$ ). Other biological processes less typically associated with EMT such as “defense response to bacterium” and “signaling by interleukins” were picked up by the analysis. However, the same cytokine and inflammatory-mediated response to bacteria can help explain another way EMT-related genes play a role in cancer progression. The increased angiogenic and metabolic changes associated with certain proinflammatory states, which would help fend off a bacterial infection, can serve as fertile ground for initiation of cancer metastasis.

Among the most salient advances in our understanding of cancer progression is the complex role the immune system plays. Notable mediators of the immune system repeatedly occurred in our analysis. TGFBR1, a receptor for the TGF $\beta$  growth factor, and CSF1R, a cytokine receptor, have been linked to pro-survival activity [62–65]. In other cancers, the chemokine CCL15 has been linked to tumor-associated macrophage recruitment and CCL18 has been linked to an immunosuppressive tumor microenvironment, allowing for evasion of the host’s immune system [66–69]. The most common immune cell type with a significant correlation was CD4+ T cells. While classically thought of as having an anti-tumor role, the varied subtypes not completely covered in our current deconvolution methods may play a paradoxical pro-tumor role. It is possible they do so by decreasing activation of other immune cells such as macrophages, warranting further study into the specific gene to immune cell interaction [70].

While this research represents a step forward in investigating the expression patterns of EMT-related genes, there exist certain limitations to these discoveries. These assessments rely on the levels of mRNA in a stable state as a proxy for protein levels. To partially address this, proteomic analysis of the highlighted genes in our study were examined in bladder cancer models through the depmap.org portal (<https://depmap.org/portal/> (accessed on 12 September 2023)) and Cancer Cell Line Encyclopedia (CCLE), verifying expression of highlighted genes. Moreover, the functional behavior of these mRNA molecules could be subject to additional regulation by post-translational elements. Additionally, the techniques used to decipher immune cell infiltrations might be influenced by the tumor’s purity,

contingent upon the specific formula employed. Ongoing efforts are dedicated to refining methods for accurately estimating cellular infiltrations based on mRNA levels. Overall, this study potentially serves as a starting point for future investigations aimed at directly scrutinizing the highlighted relationship between gene expression and prognosis, extending to the protein or enzymatic realm.

**Supplementary Materials:** The following supporting information can be downloaded at: <https://www.mdpi.com/article/10.3390/genes14101899/s1>.

**Author Contributions:** Conceptualization, W.A. and A.K.-B.; methodology, W.A.; software, A.K.-B.; validation, W.A., W.X. and D.J.; formal analysis, W.A. and D.J.; resources, W.A.; data curation, W.X.; writing—original draft preparation, W.A.; writing—review and editing, W.A. and W.X.; visualization, D.J.; supervision, A.K.-B.; project administration, A.K.-B. All authors have read and agreed to the published version of the manuscript.

**Funding:** This research received no external funding.

**Institutional Review Board Statement:** Not applicable.

**Informed Consent Statement:** Not applicable.

**Data Availability Statement:** Publicly available datasets were analyzed in this study. This data can be found through <https://www.cancer.gov/ccg/research/genome-sequencing/tcga> (accessed on 1 September 2022) or on the R2 platform as described above.

**Conflicts of Interest:** The authors declare no conflict of interest.

## Appendix A

Below is the complete list of genes listed as “immunomodulators” in the aforementioned analysis.

**Table A1.** Complete list of genes included as “immunomodulators”.

Immunomodulators	Chemokines	Chemokines
<i>ADORA2A</i>	CCL1	CX3CL1
<i>BTLA</i>	CCL2	CXCL1
<i>CD160</i>	CCL3	CXCL2
<i>CD244</i>	CCL4	CXCL3
<i>CD274</i>	CCL5	CXCL5
<i>CD96</i>	CCL7	CXCL6
<i>CSF1R</i>	CCL8	CXCL8
<i>CTLA4</i>	CCL11	CXCL9
<i>HAVCR2</i>	CCL13	CXCL10
<i>IDO1</i>	CCL14	CXCL11
<i>IL10</i>	CCL15	CXCL12
<i>IL10RB</i>	CCL16	CXCL13
<i>KDR</i>	CCL17	CXCL14
<i>KIR2DL1</i>	CCL18	CXCL16
<i>KIR2DL3</i>	CCL19	CXCL17
<i>LAG3</i>	CCL20	XCL1
<i>LGALS9</i>	CCL21	XCL2
<i>PDCD1</i>	CCL22	
<i>PDCD1LG2</i>	CCL23	
<i>PVRL2</i>	CCL24	
<i>TGFB1</i>	CCL25	
<i>TGFBR1</i>	CCL26	
<i>TIGIT</i>	CCL27	
<i>VTCN1</i>	CCL28	

**Table A2.** Spearman’s correlation data for all EMT-related genes, grouped by EMT-gene of interest. Only correlations shown to be statistically significant ( $p < 0.05$  post multiple hypothesis correction) and deemed clinically significant  $|\rho| > 0.4$  are depicted.

Gene of Interest	Immunomodulator Gene	rho
<i>TBX3</i>	<i>CXCL16</i>	−0.434
	<i>CXCL13</i>	−0.401
	<i>CXCL11</i>	−0.482
	<i>CXCL10</i>	−0.512
	<i>CXCL9</i>	−0.458
	<i>CXCL5</i>	−0.474
	<i>CXCL3</i>	−0.470
	<i>CXCL2</i>	−0.453
	<i>CXCL1</i>	−0.424
	<i>CCL26</i>	−0.489
	<i>CCL23</i>	−0.415
	<i>CCL18</i>	−0.469
	<i>CCL15</i>	0.474
	<i>CCL13</i>	−0.411
	<i>CCL8</i>	−0.535
	<i>CCL7</i>	−0.544
	<i>CCL5</i>	−0.443
	<i>CCL4</i>	−0.570
	<i>CCL3</i>	−0.571
	<i>TIGIT</i>	−0.416
	<i>TGFBR1</i>	−0.45
	<i>PDCD1LG2</i>	−0.654
	<i>PDCD1</i>	−0.4
	<i>LAG3</i>	−0.528
	<i>IL10</i>	−0.449
	<i>IDO1</i>	−0.464
	<i>HAVCR2</i>	−0.570
	<i>CTLA4</i>	−0.423
	<i>CSF1R</i>	−0.562
	<i>CD274</i>	−0.507
<i>NRP2</i>	<i>CXCL13</i>	0.454
	<i>CXCL12</i>	0.647
	<i>CXCL11</i>	0.426
	<i>CXCL10</i>	0.453
	<i>CXCL9</i>	0.490
	<i>CXCL2</i>	0.408
	<i>CCL26</i>	0.579
	<i>CCL23</i>	0.461
	<i>CCL21</i>	0.57
	<i>CCL19</i>	0.426
	<i>CCL18</i>	0.519
	<i>CCL13</i>	0.488
	<i>CCL11</i>	0.479
	<i>CCL8</i>	0.525
	<i>CCL7</i>	0.531
	<i>CCL5</i>	0.432
	<i>CCL4</i>	0.507
	<i>CCL3</i>	0.501
	<i>CCL2</i>	0.553
	<i>LAG3</i>	0.434
	<i>TIGIT</i>	0.435
	<i>TGFBR1</i>	0.550
	<i>PDCD1LG2</i>	0.676
<i>PDCD1</i>	0.438	
<i>IL10</i>	0.633	

Table A2. Cont.

Gene of Interest	Immunomodulator Gene	rho
FOXA1	HAVCR2	0.633
	CTLA4	0.460
	CSF1R	0.679
	BTLA	0.433
	ADORA2A	0.402
	CXCL12	−0.419
	CXCL11	−0.401
	CXCL10	−0.446
	CXCL9	−0.415
	CXCL5	−0.450
	CXCL3	−0.425
	CXCL2	−0.471
	CCL26	−0.555
	CCL23	−0.426
	CCL21	−0.408
	CCL18	−0.474
	CCL15	0.467
	CCL13	−0.469
	CCL8	−0.581
	CCL7	−0.589
CCL5	−0.461	
CCL4	−0.547	
CCL3	−0.594	
CCL2	−0.498	
TGFBR1	−0.442	
TGFB1	−0.414	
PDCD1LG2	−0.687	
LAG3	−0.518	
IL10	−0.520	
HAVCR2	−0.572	
CTLA4	−0.425	
CSF1R	−0.599	
CD274	−0.492	
FN1	TGFBR1	0.570
	TGFB1	0.410
	PDCD1LG2	0.716
	LAG3	0.431
	IL10	0.648
	HAVCR2	0.620
	CSF1R	0.657
	CD274	0.416
	CXCL13	0.415
	CXCL12	0.625
	CXCL11	0.404
	CXCL10	0.448
	CXCL9	0.458
	CXCL5	0.418
	CXCL2	0.401
	CCL26	0.554
	CCL23	0.459
	CCL21	0.539
	CCL18	0.551
	CCL13	0.522
CCL11	0.561	
CCL7	0.540	
CCL5	0.462	
CCL4	0.505	

Table A2. Cont.

Gene of Interest	Immunomodulator Gene	rho
FBP1	CCL3	0.511
	CCL2	0.524
	CCL15	0.592
	CCL4	−0.404
	TGFBR1	−0.455
ANXA1	PDCD1LG2	−0.491
	CD274	−0.474
	PDCD1LG2	0.504
	CD274	0.451
LAMC2	CCL15	−0.414
	CCL7	0.407
	CXCL8	0.440
HOOK1	CXCL1	0.422
	TGFB1	0.433
	TGFB1	−0.423
NES	CSF1R	−0.410
	CCL23	−0.403
	CXCL12	0.423
SPRR2A	KDR	0.405
	CXCL1	0.423
PTPN6	CXCL8	0.412
	LGALS9	0.422
RUNX2	PDCD1LG2	0.451

## References

- Bladder cancer statistics | World Cancer Research Fund International. Available online: <https://www.wcrf.org/cancer-trends/bladder-cancer-statistics/> (accessed on 7 June 2023).
- Thompson, D.B.; Siref, L.E.; Feloney, M.P.; Hauke, R.J.; Agrawal, D.K. Immunological basis in the pathogenesis and treatment of bladder cancer. *Expert. Rev. Clin. Immunol.* **2015**, *11*, 265–279. [CrossRef] [PubMed]
- Ploeg, M.; Aben, K.K.H.; Kiemeny, L.A. The present and future burden of urinary bladder cancer in the world. *World J. Urol.* **2009**, *27*, 289. [CrossRef] [PubMed]
- Wong, M.C.S.; Fung, F.D.H.; Leung, C.; Cheung, W.W.L.; Goggins, W.B.; Ng, C.F. The global epidemiology of bladder cancer: A joinpoint regression analysis of its incidence and mortality trends and projection. *Sci. Rep.* **2018**, *8*, 1129. [CrossRef] [PubMed]
- Purdue, M.P.; Hutchings, S.J.; Rushton, L.; Silverman, D.T. The proportion of cancer attributable to occupational exposures. *Ann. Epidemiol.* **2015**, *25*, 188. [CrossRef]
- Cumberbatch, M.G.; Windsor-Shellard, B.; Catto, J.W.F. The contemporary landscape of occupational bladder cancer within the United Kingdom: A meta-analysis of risks over the last 80 years. *BJU Int.* **2017**, *119*, 100–109. [CrossRef]
- Figuroa, J.D.; Ye, Y.; Siddiq, A.; Garcia-Closas, M.; Chatterjee, N.; Prokunina-olsson, L.; Cortessis, V.K.; Kooperberg, C.; Cussenot, O.; Benhamou, S.; et al. Genome-wide association study identifies multiple loci associated with bladder cancer risk. *Human Mol. Genet.* **2014**, *23*, 1387–1398. [CrossRef]
- Garcia-Closas, M.; Rothman, N.; Figuroa, J.D.; Prokunina-Olsson, L.; Han, S.S.; Baris, D.; Jacobs, E.J.; Malats, N.; De Vivo, I.; Albanes, D.; et al. Common genetic polymorphisms modify the effect of smoking on absolute risk of bladder cancer. *Cancer Res.* **2013**, *73*, 2211–2220. [CrossRef]
- Engel, L.S.; Taioli, E.; Pfeiffer, R.; Garcia-Closas, M.; Marcus, P.M.; Lan, Q.; Boffetta, P.; Vineis, P.; Autrup, H.; Bell, D.A.; et al. Pooled analysis and meta-analysis of glutathione S-transferase M1 and bladder cancer: A HuGE review. *Am. J. Epidemiol.* **2002**, *156*, 95–109. [CrossRef]
- Figuroa, J.D.; Koutros, S.; Colt, J.S.; Kogevinas, M.; Garcia-Closas, M.; Real, F.X.; Friesen, M.C.; Baris, D.; Stewart, P.; Schwenn, M.; et al. Modification of Occupational Exposures on Bladder Cancer Risk by Common Genetic Polymorphisms. *JNCI J. Natl. Cancer Inst.* **2015**, *107*, 223. [CrossRef]

11. Carlo, M.I.; Ravichandran, V.; Srinivasan, P.; Bandlamudi, C.; Kemel, Y.; Ceyhan-Birsoy, O.; Mukherjee, S.; Mandelker, D.; Chaim, J.; Knezevic, A.; et al. Cancer Susceptibility Mutations in Patients with Urothelial Malignancies. *J. Clin. Oncol. Off. J. Am. Soc. Clin. Oncol.* **2020**, *38*, 406–414. [[CrossRef](#)]
12. Malats, N.; Bustos, A.; Nascimento, C.M.; Fernandez, F.; Rivas, M.; Puente, D.; Kogevinas, M.; Real, F.X. P53 as a prognostic marker for bladder cancer: A meta-analysis and review. *Lancet Oncol.* **2005**, *6*, 678–686. [[CrossRef](#)] [[PubMed](#)]
13. Shariat, S.F.; Tokunaga, H.; Zhou, J.H.; Kim, J.H.; Ayala, G.E.; Benedict, W.F.; Lerner, S.P. p53, p21, pRB, and p16 expression predict clinical outcome in cystectomy with bladder cancer. *J. Clin. Oncol. Off. J. Am. Soc. Clin. Oncol.* **2004**, *22*, 1014–1024. [[CrossRef](#)] [[PubMed](#)]
14. Benedict, W.F.; Lerner, S.P.; Zhou, J.; Shen, X.; Tokunaga, H.; Czerniak, B. Level of retinoblastoma protein expression correlates with p16 (MTS-1/INK4A/CDKN2) status in bladder cancer. *Oncogene* **1999**, *18*, 1197–1203. [[CrossRef](#)]
15. Kader, A.K.; Shao, L.; Dinney, C.P.; Schabath, M.B.; Wang, Y.; Liu, J.; Gu, J.; Grossman, H.B.; Wu, X. Matrix metalloproteinase polymorphisms and bladder cancer risk. *Cancer Res.* **2006**, *66*, 11644–11648. [[CrossRef](#)] [[PubMed](#)]
16. Lin, J.; Spitz, M.R.; Wang, Y.; Schabath, M.B.; Gorlov, I.P.; Hernandez, L.M.; Pillow, P.C.; Grossman, H.B.; Wu, X. Polymorphisms of folate metabolic genes and susceptibility to bladder cancer: A case-control study. *Carcinogenesis* **2004**, *25*, 1639–1647. [[CrossRef](#)]
17. Kaderlik, K.R.; Kadlubar, F.F. Metabolic polymorphisms and carcinogen-DNA adduct formation in human populations. *Pharmacogenetics* **1995**, *5*, S108–S117. [[CrossRef](#)]
18. Dobruch, J.; Oszczudowski, M. Bladder Cancer: Current Challenges and Future Directions. *Medicina* **2021**, *57*, 749. [[CrossRef](#)]
19. Advanced Bladder Cancer Meta-analysis Collaboration. Neoadjuvant chemotherapy for invasive bladder cancer. *Cochrane Database Syst. Rev.* **2004**, *2004*. [[CrossRef](#)]
20. Pham, A.; Ballas, L.K. Trimodality therapy for bladder cancer: Modern management and future directions. *Curr. Opin. Urol.* **2019**, *29*, 210–215. [[CrossRef](#)]
21. Ott, P.A.; Hu-Lieskovan, S.; Chmielowski, B.; Govindan, R.; Naing, A.; Bhardwaj, N.; Margolin, K.; Awad, M.M.; Hellmann, M.D.; Lin, J.J.; et al. A Phase Ib Trial of Personalized Neoantigen Therapy Plus Anti-PD-1 in Patients with Advanced Melanoma, Non-small Cell Lung Cancer, or Bladder Cancer. *Cell* **2020**, *183*, 347–362.e324. [[CrossRef](#)]
22. Magers, M.J.; Lopez-Beltran, A.; Montironi, R.; Williamson, S.R.; Kaimakliotis, H.Z.; Cheng, L. Staging of bladder cancer. *Histopathology* **2019**, *74*, 112–134. [[CrossRef](#)] [[PubMed](#)]
23. Langbein, S.; Szakacs, O.; Wilhelm, M.; Sukosd, F.; Weber, S.; Jauch, A.; Lopez Beltran, A.; Alken, P.; Kälble, T.; Kovacs, G. Alteration of the LRP1B gene region is associated with high grade of urothelial cancer. *Lab. Investig.* **2002**, *82*, 639–643. [[CrossRef](#)] [[PubMed](#)]
24. Damrauer, J.S.; Beckabir, W.; Klomp, J.; Zhou, M.; Plimack, E.R.; Galsky, M.D.; Grivas, P.; Hahn, N.M.; O'Donnell, P.H.; Iyer, G.; et al. Collaborative study from the Bladder Cancer Advocacy Network for the genomic analysis of metastatic urothelial cancer. *Nat. Commun.* **2022**, *13*, 6658. [[CrossRef](#)]
25. Habuchi, T.; Takahashi, R.; Yamada, H.; Ogawa, O.; Kakehi, Y.; Ogura, K.; Hamazaki, S.; Toguchida, J.; Ishizaki, K.; Fujita, J.; et al. Influence of cigarette smoking and schistosomiasis on p53 gene mutation in urothelial cancer. *Cancer Res.* **1993**, *53*, 3795–3799.
26. Hou, R.; Kong, X.; Yang, B.; Xie, Y.; Chen, G. SLC14A1: A novel target for human urothelial cancer. *Clin. Transl. Oncol.* **2017**, *19*, 1438–1446. [[CrossRef](#)]
27. Zlotta, A.R.; Roumeguere, T.; Kuk, C.; Alkhateeb, S.; Rorive, S.; Lemy, A.; Van Der Kwast, T.H.; Fleshner, N.E.; Jewett, M.A.S.; Finelli, A.; et al. Select screening in a specific high-risk population of patients suggests a stage migration toward detection of non-muscle-invasive bladder cancer. *Eur. Urol.* **2011**, *59*, 1026–1031. [[CrossRef](#)] [[PubMed](#)]
28. PubMed Health. A service of the National Library of Medicine, N.I.o.H. In *Bladder Cancer Treatment (PDQ®)*. Available online: <https://www.ncbi.nlm.nih.gov/books/NBK65962/> (accessed on 7 June 2023).
29. Sylvester, R.J.; Van Der Meijden, A.P.M.; Oosterlinck, W.; Witjes, J.A.; Bouffouix, C.; Denis, L.; Newling, D.W.W.; Kurth, K. Predicting recurrence and progression in individual patients with stage Ta T1 bladder cancer using EORTC risk tables: A combined analysis of 2596 patients from seven EORTC trials. *Eur. Urol.* **2006**, *49*, 466–477. [[CrossRef](#)]
30. Friedl, P.; Mayor, R. Tuning Collective Cell Migration by Cell-Cell Junction Regulation. *Cold Spring Harb. Perspect. Biol.* **2017**, *9*, a029199. [[CrossRef](#)]
31. Nieto, M.A.; Huang, R.Y.; Jackson, R.A.; Thiery, J.P. EMT: 2016. *Cell* **2016**, *166*, 21–45. [[CrossRef](#)]
32. Friedl, P. Preshaping and plasticity: Shifting mechanisms of cell migration. *Curr. Opin. Cell Biol.* **2004**, *16*, 14–23. [[CrossRef](#)]
33. Ramesh, V.; Brabletz, T.; Ceppi, P. Targeting EMT in Cancer with Repurposed Metabolic Inhibitors. *Trends Cancer* **2020**, *6*, 942–950. [[CrossRef](#)] [[PubMed](#)]
34. Micalizzi, D.S.; Farabaugh, S.M.; Ford, H.L. Epithelial-mesenchymal transition in cancer: Parallels between normal development and tumor progression. *J. Mammary Gland. Biol. Neoplasia* **2010**, *15*, 117–134. [[CrossRef](#)] [[PubMed](#)]
35. Zhu, W.; Leber, B.; Andrews, D.W. Cytoplasmic O-glycosylation prevents cell surface transport of E-cadherin during apoptosis. *EMBO J.* **2001**, *20*, 5999–6007. [[CrossRef](#)]
36. Parsana, P.; Amend, S.R.; Hernandez, J.; Pienta, K.J.; Battle, A. Identifying global expression patterns and key regulators in epithelial to mesenchymal transition through multi-study integration. *BMC Cancer* **2017**, *17*, 447. [[CrossRef](#)]
37. Sahib, A.S.; Fawzi, A.; Zabibah, R.S.; Koka, N.A.; Khudair, S.A.; Muhammad, F.A.; Hamad, D.A. miRNA/epithelial-mesenchymal axis (EMT) axis as a key player in cancer progression and metastasis: A focus on gastric and bladder cancers. *Cell Signal.* **2023**, 110881. [[CrossRef](#)]

38. Yin, X.; Teng, X.; Ma, T.; Yang, T.; Zhang, J.; Huo, M.; Liu, W.; Yang, Y.; Yuan, B.; Yu, H.; et al. RUNX2 recruits the NuRD(MTA1)/CRL4B complex to promote breast cancer progression and bone metastasis. *Cell Death Differ.* **2022**, *29*, 2203–2217. [[CrossRef](#)] [[PubMed](#)]
39. Pranavkrishna, S.; Sanjeev, G.; Akshaya, R.L.; Rohini, M.; Selvamurugan, N. Regulation of Runx2 and Its Signaling Pathways by MicroRNAs in Breast Cancer Metastasis. *Curr. Protein Pept. Sci.* **2021**, *22*, 534–547. [[CrossRef](#)]
40. Amin, A.; Bukhari, S.; Mokhdomi, T.A.; Anjum, N.; Wafai, A.H.; Wani, Z.; Manzoor, S.; Koul, A.M.; Amin, B.; Ain, Q.U.; et al. Comparative proteomics and global genome-wide expression data implicate role of ARMC8 in lung cancer. *Asian Pac. J. Cancer Prev.* **2015**, *16*, 3691–3696. [[CrossRef](#)]
41. Xie, C.; Jiang, G.; Fan, C.; Zhang, X.; Zhang, Y.; Miao, Y.; Lin, X.; Wu, J.; Wang, L.; Liu, Y.; et al. ARMC8 $\alpha$  promotes proliferation and invasion of non-small cell lung cancer cells by activating the canonical Wnt signaling pathway. *Tumour Biol.* **2014**, *35*, 8903–8911. [[CrossRef](#)]
42. Li, X.; Zhang, C.; Yuan, Y.; Wang, Y.; Lu, S.; Zhou, Z.; Zhen, P.; Zhou, M. Downregulation of ARMC8 promotes tumorigenesis through activating Wnt/ $\beta$ -catenin pathway and EMT in cutaneous squamous cell carcinomas. *J. Dermatol. Sci.* **2021**, *102*, 184–192. [[CrossRef](#)]
43. Domanegg, K.; Sleeman, J.P.; Schmaus, A. CEMIP, a Promising Biomarker That Promotes the Progression and Metastasis of Colorectal and Other Types of Cancer. *Cancers* **2022**, *14*, 5093. [[CrossRef](#)] [[PubMed](#)]
44. Hua, Q.; Zhang, B.; Xu, G.; Wang, L.; Wang, H.; Lin, Z.; Yu, D.; Ren, J.; Zhang, D.; Zhao, L.; et al. CEMIP, a novel adaptor protein of OGT, promotes colorectal cancer metastasis through glutamine metabolic reprogramming via reciprocal regulation of  $\beta$ -catenin. *Oncogene* **2021**, *40*, 6443–6455. [[CrossRef](#)] [[PubMed](#)]
45. Rodrigues, G.; Hoshino, A.; Kenific, C.M.; Matei, I.R.; Steiner, L.; Freitas, D.; Kim, H.S.; Oxley, P.R.; Scandariato, I.; Casanova-Salas, I.; et al. Tumour exosomal CEMIP protein promotes cancer cell colonization in brain metastasis. *Nat. Cell Biol.* **2019**, *21*, 1403–1412. [[CrossRef](#)] [[PubMed](#)]
46. Liu, H.; Paddock, M.N.; Wang, H.; Murphy, C.J.; Geck, R.C.; Navarro, A.J.; Wulf, G.M.; Elemento, O.; Haucke, V.; Cantley, L.C.; et al. The INPP4B Tumor Suppressor Modulates EGFR Trafficking and Promotes Triple-Negative Breast Cancer. *Cancer Discov.* **2020**, *10*, 1226–1239. [[CrossRef](#)] [[PubMed](#)]
47. Arruabarrena-Aristorena, A.; Maag, J.L.V.; Kittane, S.; Cai, Y.; Karthaus, W.R.; Ladewig, E.; Park, J.; Kannan, S.; Ferrando, L.; Cocco, E.; et al. FOXA1 Mutations Reveal Distinct Chromatin Profiles and Influence Therapeutic Response in Breast Cancer. *Cancer Cell* **2020**, *38*, 534–550.e539. [[CrossRef](#)] [[PubMed](#)]
48. Jäggle, S.; Busch, H.; Freißen, V.; Beyes, S.; Schrempp, M.; Boerries, M.; Hecht, A. SNAIL1-mediated downregulation of FOXA proteins facilitates the inactivation of transcriptional enhancer elements at key epithelial genes in colorectal cancer cells. *PLoS Genet.* **2017**, *13*, e1007109. [[CrossRef](#)] [[PubMed](#)]
49. Dong, L.; Lyu, X.; Faleti, O.D.; He, M.L. The special stemness functions of Tbx3 in stem cells and cancer development. *Semin. Cancer Biol.* **2019**, *57*, 105–110. [[CrossRef](#)]
50. Khan, S.F.; Burmeister, C.A.; Scott, D.J.; Sinkala, M.; Ramburan, A.; Wu, H.T.; Schäfer, G.; Katz, A.A.; Prince, S. TBX3 Promotes Cervical Cancer Proliferation and Migration via HPV E6 and E7 Signaling. *Mol. Cancer Res.* **2023**, *21*, 345–358. [[CrossRef](#)]
51. Liang, B.; Zhou, Y.; Qian, M.; Xu, M.; Wang, J.; Zhang, Y.; Song, X.; Wang, H.; Lin, S.; Ren, C.; et al. TBX3 functions as a tumor suppressor downstream of activated CTNNB1 mutants during hepatocarcinogenesis. *J. Hepatol.* **2021**, *75*, 120–131. [[CrossRef](#)]
52. Shen, C.; Liu, J.; Wang, J.; Yang, X.; Niu, H.; Wang, Y. The Analysis of PTPN6 for Bladder Cancer: An Exploratory Study Based on TCGA. *Dis. Markers* **2020**, *2020*, 4312629. [[CrossRef](#)]
53. Liu, G.; Zhang, Y.; Huang, Y.; Yuan, X.; Cao, Z.; Zhao, Z. PTPN6-EGFR Protein Complex: A Novel Target for Colon Cancer Metastasis. *J. Oncol.* **2022**, *2022*, 7391069. [[CrossRef](#)] [[PubMed](#)]
54. Zhu, X.; Zhou, L.; Li, R.; Shen, Q.; Cheng, H.; Shen, Z.; Zhu, H. AGER promotes proliferation and migration in cervical cancer. *Biosci. Rep.* **2018**, *38*, BSR20171329. [[CrossRef](#)] [[PubMed](#)]
55. Tang, Y.; Li, M.; Wang, Y.L.; Threadgill, M.D.; Xiao, M.; Mou, C.F.; Song, G.L.; Kuang, J.; Yang, X.; Yang, L.; et al. ART1 promotes starvation-induced autophagy: A possible protective role in the development of colon carcinoma. *Am. J. Cancer Res.* **2015**, *5*, 498–513. [[PubMed](#)]
56. Melincovici, C.S.; Boşca, A.B.; Şuşman, S.; Mărginean, M.; Mişu, C.; Istrate, M.; Moldovan, I.M.; Roman, A.L.; Mişu, C.M. Vascular endothelial growth factor (VEGF)-key factor in normal and pathological angiogenesis. *Rom. J. Morphol. Embryol.* **2018**, *59*, 455–467. [[PubMed](#)]
57. Xu, K.; Wu, C.L.; Wang, Z.X.; Wang, H.J.; Yin, F.J.; Li, W.D.; Liu, C.C.; Fan, H.N. VEGF Family Gene Expression as Prognostic Biomarkers for Alzheimer’s Disease and Primary Liver Cancer. *Comput. Math. Methods Med.* **2021**, *2021*, 3422393. [[CrossRef](#)]
58. Taha, F.M.; Zeeneldin, A.A.; Helal, A.M.; Gaber, A.A.; Sallam, Y.A.; Ramadan, H.; Moneer, M.M. Prognostic value of serum vascular endothelial growth factor in Egyptian females with metastatic triple negative breast cancer. *Clin. Biochem.* **2009**, *42*, 1420–1426. [[CrossRef](#)]
59. Charles Jacob, H.K.; Signorelli, R.; Charles Richard, J.L.; Kashuv, T.; Lavania, S.; Middleton, A.; Gomez, B.A.; Ferrantella, A.; Amirian, H.; Tao, J.; et al. Identification of novel early pancreatic cancer biomarkers KIF5B and SFRP2 from “first contact” interactions in the tumor microenvironment. *J. Exp. Clin. Cancer Res.* **2022**, *41*, 258. [[CrossRef](#)]
60. Müller, D.; Györfy, B. DNA methylation-based diagnostic, prognostic, and predictive biomarkers in colorectal cancer. *Biochim. Biophys. Acta Rev. Cancer* **2022**, *1877*, 188722. [[CrossRef](#)]

61. Goetz, J.G.; Lajoie, P.; Wiseman, S.M.; Nabi, I.R. Caveolin-1 in tumor progression: The good, the bad and the ugly. *Cancer Metastasis Rev.* **2008**, *27*, 715–735. [[CrossRef](#)]
62. Kretzschmar, M.; Doody, J.; Timokhina, I.; Massagué, J. A mechanism of repression of TGFbeta/ Smad signaling by oncogenic Ras. *Genes Dev.* **1999**, *13*, 804–816. [[CrossRef](#)]
63. Ranganathan, P.; Agrawal, A.; Bhushan, R.; Chavalmane, A.K.; Kalathur, R.K.; Takahashi, T.; Kondaiiah, P. Expression profiling of genes regulated by TGF-beta: Differential regulation in normal and tumour cells. *BMC Genom.* **2007**, *8*, 98. [[CrossRef](#)] [[PubMed](#)]
64. Murga-Zamalloa, C.; Rolland, D.C.M.; Polk, A.; Wolfe, A.; Dewar, H.; Chowdhury, P.; Onder, O.; Dewar, R.; Brown, N.A.; Bailey, N.G.; et al. Colony-Stimulating Factor 1 Receptor (CSF1R) Activates AKT/mTOR Signaling and Promotes T-Cell Lymphoma Viability. *Clin. Cancer Res.* **2020**, *26*, 690–703. [[CrossRef](#)] [[PubMed](#)]
65. Wen, J.; Wang, S.; Guo, R.; Liu, D. CSF1R inhibitors are emerging immunotherapeutic drugs for cancer treatment. *Eur. J. Med. Chem.* **2023**, *245*, 114884. [[CrossRef](#)] [[PubMed](#)]
66. Gao, Y.; Zhou, Z.; Lu, S.; Huang, X.; Zhang, C.; Jiang, R.; Yao, A.; Sun, B.; Wang, X. Chemokine CCL15 Mediates Migration of Human Bone Marrow-Derived Mesenchymal Stem Cells Toward Hepatocellular Carcinoma. *Stem Cells* **2016**, *34*, 1112–1122. [[CrossRef](#)]
67. Yin, X.; Han, S.; Song, C.; Zou, H.; Wei, Z.; Xu, W.; Ran, J.; Tang, C.; Wang, Y.; Cai, Y.; et al. Metformin enhances gefitinib efficacy by interfering with interactions between tumor-associated macrophages and head and neck squamous cell carcinoma cells. *Cell Oncol.* **2019**, *42*, 459–475. [[CrossRef](#)]
68. Azzaoui, I.; Yahia, S.A.; Chang, Y.; Vorng, H.; Morales, O.; Fan, Y.; Delhem, N.; Ple, C.; Tonnel, A.B.; Wallaert, B.; et al. CCL18 differentiates dendritic cells in tolerogenic cells able to prime regulatory T cells in healthy subjects. *Blood* **2011**, *118*, 3549–3558. [[CrossRef](#)]
69. Martinez, F.O.; Gordon, S.; Locati, M.; Mantovani, A. Transcriptional profiling of the human monocyte-to-macrophage differentiation and polarization: New molecules and patterns of gene expression. *J. Immunol.* **2006**, *177*, 7303–7311. [[CrossRef](#)]
70. Ben Khelil, M.; Godet, Y.; Abdeljaoued, S.; Borg, C.; Adotévi, O.; Loyon, R. Harnessing Antitumor CD4(+) T Cells for Cancer Immunotherapy. *Cancers* **2022**, *14*, 260. [[CrossRef](#)]

**Disclaimer/Publisher’s Note:** The statements, opinions and data contained in all publications are solely those of the individual author(s) and contributor(s) and not of MDPI and/or the editor(s). MDPI and/or the editor(s) disclaim responsibility for any injury to people or property resulting from any ideas, methods, instructions or products referred to in the content.